

Dynamical frictional phenomena in an incommensurate two-chain model

Takaaki Kawaguchi

*Department of Technology, Faculty of Education, Shimane University
1060 Nishikawatsu, Matsue 690, Japan*

Hiroshi Matsukawa

*Department of Physics, Osaka University
1-16 Machikaneyama Toyonaka, Osaka 560, Japan*

Dynamical frictional phenomena are studied theoretically in a two-chain model with incommensurate structure. A perturbation theory with respect to the interchain interaction reveals the contributions from phonons excited in each chain to the kinetic frictional force. The validity of the theory is verified in the case of weak interaction by comparing with numerical simulation. The velocity and the interchain interaction dependences of the lattice structure are also investigated. It is shown that peculiar breaking of analyticity states appear, which is characteristic to the two-chain model. The range of the parameters in which the two-chain model is reduced to the Frenkel-Kontorova model is also discussed.

81.40.Pq, 46.30.Pa

I. INTRODUCTION

The sliding velocity dependence of the kinetic frictional force is of particular importance in the field of tribology. The Coulomb-Amontons law states that the kinetic frictional force does not depend on the sliding velocity [1]. It is well known that this law holds well under usual condition, but breaks in some cases. Its physical explanation is not well-established. In recent years the study of atomic scale frictional phenomena has been a hot issue [2–5]. In such microscopic systems, new physical laws and concepts of friction is considered to exist. Several works on kinetic friction have been reported using microscopic or atomic scale models [5]. Among these studies, the Frenkel-Kontorova model (FK model) [6] and related ones have been investigated extensively by several researchers [7–17]. The FK model consists of the atoms interacting each other via harmonic force under a periodic potential. In the case that the ratio between the mean atomic spacing and the period of the potential is irrational, i.e., in an incommensurate case, the FK model shows a phase transition, the so-called Aubry transition [7,8]. When the amplitude of the periodic potential is smaller than a certain critical value, the maximum static frictional force vanishes. Above the critical amplitude it becomes finite. The dynamical properties of the FK and related models have been reported by many authors. Coppersmith and Fisher investigated the behavior near the maximum static frictional force in the FK model from the viewpoint of critical phenomena [9,10]. Then, the critical exponent of the velocity-force characteristics was evaluated. Sokoloff developed a perturbation theory of frictional force [11]. He employed a three-dimensional FK model, which consists of a three-dimensional deformable lattice and a rigid substrate, which makes pe-

riodic potential. He discussed frictional effects in commensurate and incommensurate systems and found that strong reduction of kinetic frictional force for an incommensurate system compared with that for a commensurate one. The existence of a superlubricity state, in which the frictional force vanishes, was claimed by Hirano and Shinjo in a three-dimensional FK model [12,13]. Since they assumed an energy conservative system, the kinetic frictional force vanishes by the energy recurrence effect between the motion of the center of gravity and the lattice vibration. Matsukawa and Fukuyama investigated the static and kinetic frictional forces based on a one-dimensional model [14,17]. The model employed in their study consists of two atomic chains, where the interchain interaction, the harmonic intrachain interaction and the effect of energy dissipation are taken into account. In their model a definitive expression of both of static and kinetic frictional forces can be derived. Using a numerical simulation, they found that the critical amplitude of interchain potential where the Aubry transition occurs depends strongly on the elasticity of the chains. They investigated also the velocity dependence of the kinetic frictional force. When the interchain interaction is weak, the crossover behavior of the kinetic frictional force between velocity-strengthening to velocity-weakening is observed as velocity increases. It was also found that the crossover velocity and the strength of the kinetic frictional force make obvious difference whether the lower chain is deformable or rigid. For strong interchain interaction, the velocity-strengthening behavior is smeared out because of large maximum static frictional force. Quasi-periodic and chaotic sliding states were discussed by Elmer, Strunz and Weiss in the underdamped regime of the FK and FK-Tomlinson models [16].

For the theoretical understanding of the dynamics of

frictional phenomena, it is desirable to clarify the behavior and features of kinetic frictional force both by numerical and analytical methods. In this paper, using the one-dimensional two-chain model of friction proposed in Ref. [14], we revisit the dynamic properties of the model and calculate the kinetic frictional force by employing both of perturbation theory and numerical calculation. On the basis of a theoretical expression of frictional force [14], we can successfully formulate the perturbation theory on the calculation of the kinetic frictional force for the two-chain model. The role of the phonon excited in each chain can be clarified. Numerical simulations are employed to clarify the validity of the perturbation theory and to investigate the atomic configuration and motion. The velocity dependence of the kinetic frictional force under various conditions is investigated. The physical meaning of the earlier results [14] on the kinetic friction is discussed. We also investigate the hull function, which characterizes the lattice structure. It is found that peculiar breaking of analyticity states appear, which is characteristic to the case of two deformable chains. Lastly we discuss the difference between the two-chain model and the FK model and the parameter regime in which the two-chain model is reduced to the FK model approximately.

II. TWO-CHAIN MODEL OF FRICTION

The two-chain model of friction is reviewed in the following. We consider two atomic chains, i.e., an upper chain and a lower chain. The atoms in each chain have one-dimensional degree of freedom parallel to the chain and interact each other via the harmonic force. Inter-chain interaction works between atoms in the upper chain and those in the lower one. The effects of energy dissipation in both chains are assumed to be proportional to the difference between the velocity of each atom and that of the center of gravity. The upper chain is subject to the external force parallel to the chain. Here we assume overdamped motion, and then the equations of motion of the atoms in the upper and lower chains are expressed as,

$$m_a \gamma_a (\dot{u}_i - \langle \dot{u}_i \rangle_i) = K_a (u_{i+1} + u_{i-1} - 2u_i) + \sum_{j \in b}^{N_b} F_I(u_i - v_j) + F_{ex}, \quad (1)$$

$$m_b \gamma_b (\dot{v}_i - \langle \dot{v}_i \rangle_i) = K_b (v_{i+1} + v_{i-1} - 2v_i) + \sum_{j \in a}^{N_a} F_I(v_i - u_j) - K_s (v_i - ic_b), \quad (2)$$

where u_i (v_i), m_a (m_b), γ_a (γ_b), K_a (K_b) and N_a (N_b) are the position of the i -th atom, the atomic mass, the parameter of energy dissipation, the strength of the interatomic force and the number of atoms in the upper

(lower) chain, respectively. K_s is the strength of the interatomic force between the lower chain and the substrate and $\langle \dots \rangle_i$ represents the average with respect to i . F_I and F_{ex} are the interchain force between the two atomic chains and the external force, respectively. We adopt the following interatomic potential:

$$U_I = -\frac{K_I}{2} \exp \left[-4 \left(\frac{x}{c_b} \right)^2 \right], \quad (3)$$

where K_I is the strength of the interchain potential, c_b the mean atomic spacing of the lower chain. The interatomic force is given by $F_I(x) = -\frac{d}{dx} U_I$. The time-averaged total frictional force of the present model is given by the following equation.

$$F^{\text{fric}} = - \sum_{i \in a}^{N_a} \sum_{j \in b}^{N_b} \langle F_I(v_i - u_j) \rangle_t = N_a \langle F_{ex} \rangle_t \quad (4)$$

It should be noted that the above expression of the frictional force is valid for both static and kinetic ones. In this study we apply Eq. (4) to the evaluation of kinetic frictional force.

III. PERTURBATION THEORY OF FRICTIONAL FORCE FOR TWO-CHAIN MODEL

We construct a perturbation theory for the kinetic frictional force that arises between two interacting atomic chains. In a steady state the upper chain is assumed to be sliding at a constant velocity, V , on average. Then the atomic positions in the upper and lower chains are expressed as,

$$u_i = Vt + ic_a + \delta u_i, \quad (5)$$

$$v_i = ic_b + \delta v_i, \quad (6)$$

where c_a (c_b) and δu_i (δv_i) denote the mean lattice spacing and the deviation of atomic position from regular site in the upper(lower) chain, respectively. By substituting them into Eq. (4), we can expand the equation in terms of δu_i and δv_i ,

$$\begin{aligned} & \sum_{i \in a}^{N_a} \sum_{j \in b}^{N_b} \langle F_I(u_i - v_j) \rangle_t \\ &= \sum_{i \in a}^{N_a} \sum_{j \in b}^{N_b} \langle F_I(Vt + ic_a + \delta u_i - jc_b - \delta v_j) \rangle_t \\ &\approx \sum_{i \in a}^{N_a} \sum_{j \in b}^{N_b} [\langle F_I(Vt + ic_a - jc_b) \rangle_t \\ &+ \langle \frac{\partial}{\partial u_i} F_I(u_i - v_j) \rangle_{u_i=Vt+ic_a, v_j=jc_b} \delta u_i \rangle_t \\ &+ \langle \frac{\partial}{\partial v_j} F_I(u_i - v_j) \rangle_{u_i=Vt+ic_a, v_j=jc_b} \delta v_j \rangle_t]. \quad (7) \end{aligned}$$

In this equation the first term vanishes because the present model has an incommensurate lattice structure and then the summations with respect to i and j cancel out. The second term represents the contribution from the phonon excited in the upper chain when the atoms in the lower chain are fixed at the regular sites. On the other hand, the third term represents the contribution from the phonon excited in the lower chain when the upper chain is rigid, but moving at a constant velocity V relative to the lower chain. Then the frictional force is simply given by the sum of both the lowest-order terms. Because atomic displacements δu_i and δv_i are caused by the interchain interaction, the calculation of the frictional force in the lowest order perturbation, Eq. (7), assumes that $\delta u_i \neq 0$ and $\delta v_i = 0$ in the second term, and $\delta u_i = 0$ and $\delta v_i \neq 0$ in the third term, respectively. The contributions from terms in which both δu_i and δv_i are nonzero arise from higher order perturbations.

First of all, we examine the second term in Eq. (7). It is of particular interest because the friction in the FK model is given by this term as discussed just below. The force that acts on an atom in the upper chain in the leading order of δv_j is expressed by the following Fourier series.

$$\sum_{j \in b}^{N_b} F_I(u_i - v_j) \Big|_{v_j = jc_b} \approx -0.47K_I \sin\left(2\pi \frac{u_i}{c_b}\right) - 0.00057K_I \sin\left(4\pi \frac{u_i}{c_b}\right). \quad (8)$$

Hence, we can successfully neglect the second term in Eq. (8). Then, the equation of motion of the upper chain in the present perturbation theory approximately corresponds to the following equation of motion.

$$m_a \gamma_a \delta \dot{u}_i = K_a \{\delta u_{i+1} + \delta u_{i-1} - 2\delta u_i\} - 0.47K_I \sin\left[\frac{2\pi}{c_b}(Vt + ic_a + \delta u_i)\right]. \quad (9)$$

This is nothing but the overdamped equation of motion of the FK model.

In the perturbation theory [11,18], the atomic displacement is expressed by the recursive equation,

$$\delta u_i = \frac{0.47K_I}{m_a} \sum_j^{N_a} \int dt' G_{ij}(t-t') \left\{ \sin\left[\frac{2\pi}{c_b}(Vt' + jc_a + \delta u_j)\right] - \left\langle \sin\left[\frac{2\pi}{c_b}(Vt + ic_a + \delta u_i)\right] \right\rangle_{i,t} \right\}, \quad (10)$$

where $G_{ij}(t-t')$ is the Green function of phonons defined as

$$G_{ij}(t) = \frac{1}{N_a} \sum_k \int \frac{d\omega}{2\pi} G_k(\omega) e^{ik(i-j)c_a + i\omega t}, \quad (11)$$

$$G_k(\omega) = (i\gamma_a \omega + \Omega(k)^2)^{-1}, \quad (12)$$

$$\Omega(k)^2 = \frac{2K_a}{m_a} (1 - \cos kc_a). \quad (13)$$

In the lowest order, Eq. (10) is reduced to

$$\delta u_i \approx 0.47 \frac{K_I}{m_a} \sum_j^{N_a} \int dt' G_{ij}(t-t') \sin\left[\frac{2\pi}{c_b}(Vt' + jc_a)\right]. \quad (14)$$

Then the kinetic frictional force per atom in the upper chain resulting from the phonon excitation there, F^{upper} , is given in the lowest order of K_I as,

$$F^{\text{upper}} \approx -0.47K_I \frac{2\pi}{c_b} \frac{1}{N_a} \sum_i^{N_a} \left\langle \cos\left[\frac{2\pi}{c_b}(Vt + ic_a)\right] \delta u_i \right\rangle_t \approx \frac{(0.47K_I)^2}{2\gamma_a m_a} \frac{\left(\frac{2\pi\gamma_a}{c_b}\right)^2 V}{\Omega\left(\frac{2\pi}{c_b}\right)^4 + \left(\frac{2\pi\gamma_a V}{c_b}\right)^2}. \quad (15)$$

As easily seen by this equation there exists the crossover behavior of the velocity dependence of the kinetic frictional force between the velocity-strengthening and velocity-weakening. This is the essential feature of the kinetic frictional force in the case of small interchain interaction in the present model, which is observed in the numerical simulation in Ref. [14] and in section V. The crossover velocity is determined by three characteristic quantities: the phonon frequency at the wavenumber corresponding to the period of the underlying potential, the so-called washboard frequency $2\pi V/c_b$ and the damping constant. In order to consider the reason of this crossover behavior, it is interesting to see the average of the squared velocity fluctuation, $\langle \delta \dot{u}_i(t)^2 \rangle_{i,t}$ given by,

$$\langle \delta \dot{u}_i(t)^2 \rangle_{i,t} = 2 \left(\frac{0.47K_I}{m_a}\right)^2 \frac{\left(\frac{2\pi V}{c_b}\right)^2}{\Omega\left(\frac{2\pi}{c_b}\right)^4 + \left(\frac{2\pi\gamma_a V}{c_b}\right)^2}. \quad (16)$$

The squared velocity fluctuation shows velocity-strengthening behavior in the low velocity regime and then saturates. The former behavior comes from the increase of V , itself. The latter one results from the suppression of the fluctuation of position, $\langle \delta u_i(t)^2 \rangle_{i,t}$, in the large velocity regime, as mentioned below. We note here that the kinetic friction in the present model is caused by the energy dissipation due to the damping of the phonons excited by the sliding motion. Hence the energy dissipation per unit time in the upper chain, $F^{\text{upper}}V$, is equal to $m_a \gamma_a \langle \delta \dot{u}_i(t)^2 \rangle_{i,t}$. Then the frictional force, which is the energy dissipation per unit sliding distance, is equal to $m_a \gamma_a \langle \delta \dot{u}_i(t)^2 \rangle_{i,t} / V$. So the velocity-strengthening behavior of F^{upper} in the low velocity regime comes from that of $\langle \delta \dot{u}_i(t)^2 \rangle_{i,t}$. As V becomes

greater than $\frac{c_b}{2\pi\gamma_a}\Omega\left(\frac{2\pi}{c_b}\right)^2$, $\langle\delta u_i(t)^2\rangle_{i,t}$ saturates and then the frictional force decreases.

Next we consider the kinetic friction resulting from the phonon excitation in the lower chain. In this case we can express the interatomic force that act on an atom in the lower chain using a Fourier series as follows.

$$\sum_{i \in a}^{N_a} F_I(u_i - v_j) \Big|_{u_i = Vt + ic_a} \approx -0.83K_I \sin\left(2\pi \frac{v_j - Vt}{c_a}\right) - 0.098K_I \sin\left(4\pi \frac{v_j - Vt}{c_a}\right). \quad (17)$$

We can neglect the second term. The strength of inter-chain interaction is not equal to that in Eq. (8). This comes from the spatial profile of the interchain potential and the summation on the upper lattice site. Then the equation of motion is given by

$$m_b\gamma_b\delta\dot{v}_i = K_b\{\delta v_{i+1} + \delta v_{i-1} - 2\delta v_i\} - K_s\delta v_i - 0.83K_I \frac{2\pi}{c_a} \cos\left[\frac{2\pi}{c_a}(-Vt + ic_b)\right] \delta v_i. \quad (18)$$

After a similar calculation to that of F^{upper} , we get the kinetic frictional force resulting from the phonon excitation in the lower chain. It is written as F^{lower} and is given by

$$F^{\text{lower}} = \frac{N_b}{N_a} \frac{(0.83K_I)^2}{2\gamma_b m_b} \frac{\left(\frac{2\pi\gamma_b}{c_a}\right)^2 V}{\Omega_b \left(\frac{2\pi\gamma_b}{c_a}\right)^4 + \left(\frac{2\pi\gamma_b}{c_a} V\right)^2}, \quad (19)$$

where $\Omega_b(k) = \sqrt{(K_s + 2K_b(1 - \cos kc_b))/m_b}$ is the phonon frequency of the lower lattice. F^{lower} is also evaluated per atom in the upper chain.

The total kinetic frictional force F^{fric} is given as $F^{\text{fric}} = F^{\text{upper}} + F^{\text{lower}}$. Then the strength and velocity dependence of the total kinetic frictional force are determined by both of F^{upper} and F^{lower} . This is the essential difference with the FK model. In the latter $F^{\text{fric}} = F^{\text{upper}}$, of course.

The perturbation theory is expected to be valid under the condition that the atomic displacement of the lattices is small compared to the mean lattice spacing. That condition is expressed as follows.

$$\sqrt{\langle\delta u_i(t)^2\rangle_{i,t}} = \frac{0.47K_I}{\sqrt{2m_a}} \frac{1}{\sqrt{\Omega\left(\frac{2\pi}{c_b}\right)^4 + \left(\frac{2\pi\gamma_a}{c_b}V\right)^2}} \ll c_a, \quad (20)$$

and

$$\sqrt{\langle\delta v_i(t)^2\rangle_{i,t}} = \frac{0.83K_I}{\sqrt{2m_b}} \frac{1}{\sqrt{\Omega_b\left(\frac{2\pi}{c_a}\right)^4 + \left(\frac{2\pi\gamma_b}{c_a}V\right)^2}} \ll c_b. \quad (21)$$

These inequalities depend on velocity because atomic displacements are suppressed by large velocity. The reason is that in the equation of motion, Eqs. (1) and (2), the effect of the high-velocity-sliding motion of atoms effectively weakens that of interchain interaction, which causes the atomic displacement. It is a dynamical effect in sliding. Here we make some comments on these conditions required for the two chains. For the perturbation in the FK model, only one inequality, Eq. (20), is required, but in the two-chain model both inequalities must be satisfied simultaneously. It is to be noted that in the present lowest order calculation the total kinetic frictional force is the sum of the contributions of phonons in the upper and lower chains as mentioned above. If the conditions Eqs. (20) and (21) are broken, there appears the cross term of δu_i and δv_i , which expresses the contribution from the interaction of phonons of both chains.

IV. METHOD OF NUMERICAL SIMULATION

We perform a numerical calculation of the kinetic frictional force and examine the validity of the perturbation theory developed in the previous section. The equations of motion are numerically solved using the Runge-Kutta formula at the fourth order. We assume periodic boundary conditions in both chains. Hence the ratio of the mean lattice spacings of the upper and lower chains c_a/c_b is equal to the ratio N_b/N_a . We choose the ratio by using the continued-fraction expansion of the golden mean.

$$\frac{c_a}{c_b} = \frac{N_b}{N_a} = \frac{144}{89} = 1.617\dots, \quad (22)$$

where the expansion is truncated at the tenth order. We set the values of the model parameters as

$$N_a = 89, N_b = 144, c_a = \frac{144}{89}, c_b = 1, m_a = m_b = 1, K_a = 1, K_b = 0, \gamma_a = \gamma_b = 1, \quad (23)$$

where the intrachain force is neglected, i.e., $K_b = 0$, for simplicity. Such simplification was employed also in the earlier study [14]. The lower chain, therefore, consists of individually oscillating atoms, that is, the Einstein's model of lattice vibration is adopted in the lower lattice.

Throughout this study, the frictional force is evaluated per atom in the upper chain.

V. COMPARISON BETWEEN THE RESULTS OF THE PERTURBATION THEORY AND NUMERICAL CALCULATION

In Section III we have presented the kinetic frictional force calculated in the lowest order perturbation. Higher order terms of the perturbation can be calculated in a

similar manner, but it is easier and more straightforward here to check the validity of the lowest order perturbation by comparing its result with that of numerical calculation. First of all, we must investigate the relationship between the strength of the interchain interaction and the validity of the perturbation theory in the case that the lower chain is fixed, which corresponds to the FK model as mentioned in Section III. In this case the contribution to the kinetic frictional force results only from the phonon excitation in the upper chain. Even in such a single deformable chain case the validity of the perturbation theory has never been examined so far especially for strong interchain interaction. The kinetic frictional force in the case of weak interchain interaction, $K_I = 0.1$, which is less than the critical value of the Aubry transition, is shown in Fig. 1(a) as a function of the sliding velocity. Then the maximum static frictional force vanishes because of the absence of the Aubry transition. A good agreement between the result of the lowest order perturbation theory and that of the numerical calculation is obtained and the velocity-strengthening and velocity-weakening features are clearly observed. From this result, it is confirmed that the result of the lowest order perturbation theory is quite good. This is consistent with the condition, Eq. (20), which gives $\sqrt{\langle \delta u_i(t)^2 \rangle_{i,t}} \approx 0.01 \ll c_a$ even in the case of vanishing velocity. Hence it is found that dominant contribution to the kinetic frictional force comes from the lowest order, and then higher order terms are negligible. On the other hand, for strong interchain interaction, $K_I = 1$, which is greater than the critical value of the Aubry transition and therefore finite static frictional force exists as observed in Fig. 1(b), obvious discrepancy is observed between the result of the perturbation theory and that of the numerical calculation in the low velocity regime. This discrepancy appears to arise from the Aubry transition. The effect of the Aubry transition affects seriously the kinetic friction in the low velocity sliding state. However, we should note that in the high velocity regime ($V \geq 0.6$) the result of the lowest order perturbation and that of the numerical calculation agree well. This is also consistent with Eq. (20). The solid lines in Fig. 1 denote $\sqrt{\langle \delta u_i(t)^2 \rangle_{i,t}}/c_a$. As seen from Fig. 1(b), the frictional force derived from the lowest order perturbation theory agrees well with that from numerical calculation, where the velocity is so large that $\sqrt{\langle \delta u_i(t)^2 \rangle_{i,t}} \ll c_a$ is satisfied. Therefore, in this velocity regime, it is considered that the sliding state is well described by the lowest order perturbation theory. In the following, we analyze the lattice structure of the sliding chain and clarify that the discrete features of the atomic distribution caused by the Aubry transition is relevant to the above discrepancy in the low velocity regime.

In order to show that the validity of the perturbation

theory has a close relationship to the lattice structure of the sliding chain, it would be useful to consider the hull function, $h(x)$. It is defined as follows,

$$u_i = ic_a + h(ic_a). \quad (24)$$

The hull function is a periodic function, the period of which is that of the potential: $h(x) = h(x + c_b)$, and therefore the variable of the hull function is defined in the range from 0 to c_b . We pay our attention first to the static case ($V = 0$). When the strength of the interchain interaction is less than the critical value of the Aubry transition, the hull function is continuous and almost sinusoidal. This reflects the sinusoidal form of the interchain force of Eq. (8). Otherwise, however, the hull function is discontinuous and has gaps at several positions because of the breaking of analyticity due to the Aubry transition [7,8] as shown in Fig. 2(a). In particular, among the gaps, the largest gap is located at the half of the period, $c_b/2$. This largest central gap is considered to characterize the Aubry transition and means that the atomic distribution vanishes at the potential maximums and the atoms are bound strongly near the potential minimums. We show here that the hull function gives us an interesting insight about the atomic motion in sliding under the influence of the underlying potential as noticed in Ref. [19]. Using such a dynamical hull function, the atomic position in sliding is given by $u_i = ic_a + Vt + h(ic_a + Vt)$. Figs. 2(b)~(e) show some snapshots of the hull function at various steady sliding velocities for the strong interchain interaction, $K_I = 1$. When the velocity is small enough (Fig. 2(b)), the remainder of the gaps is clearly observed and the shape is highly distorted. It is due to the large lattice distortion caused by the Aubry transition, which is responsible for finite static frictional force. The lattice still remains highly distorted even in a sliding state. Such sliding state is characterized by the almost discontinuous and nonuniform spatial distribution of atoms which is caused by local atomic stick-slip motion in which most atoms stay nearby the potential minimums and other atoms jump over the potential maximums. It should be noted that such slip motion, of course, needs finite time and then the hull function has no gap in the case of finite velocity. In Fig. 2(b) the reminders of some small gaps are vanishing, but that of the largest gap is apparent. The deviation of the position of the remainder of the largest gap from the half of the period is due to the external force added to the sinusoidal interchain force [20]. Because the effect of large lattice distortion due to the Aubry transition is not taken into consideration in the present perturbation theory, it fails to explain the behavior of the total kinetic frictional force F^{fric} obtained by the simulation. As the velocity increases, the amplitude of the hull function decreases and its form becomes smoother and comes close to the sinusoidal one. This means that the large lattice distortion is suppressed in

the high velocity regime. In this regime the perturbation theory gives F^{fric} which agrees well with that by the simulation. As mentioned before, the suppression effect can be confirmed directly from Eq. (20), as shown by the solid lines in Fig. 1. Even when the lattice structure is subject to the Aubry transition, the dynamic suppression effect washes out it in the high velocity regime and leads to the sliding state that is described by the lowest order perturbation theory.

It turns out that the frictional property of the single deformable chain on a periodic potential can be understood on the basis of the lowest order perturbation theory. We move on to the two-chain model. We clarify the validity of the lowest order perturbation theory also here and where is the difference between the two-chain and the FK models. Figs. 3(a) and (b) show the kinetic frictional force for $K_s = 2$ and 10 respectively in the case of weak interchain interaction, $K_I = 0.1$. In these cases the maximum static frictional force is vanishing and the velocity-strengthening and velocity-weakening features of the kinetic frictional force are observed. The contributions to the kinetic frictional force from the phonon excitations in the upper and lower chains, F^{upper} and F^{lower} , and the total kinetic frictional force, F^{fric} , calculated by the perturbation theory are also plotted in these figures. For $K_s = 2$ (Fig. 3(a)), the contribution to the kinetic frictional force from the lower chain is dominant in the overall velocity regime. On the other hand, when the lower chain becomes stiffer, $K_s = 10$ (Fig. 3(b)), the contributions from both chains become important. Because the crossover velocity between velocity-strengthening and velocity-weakening features is different for each chain in this case, the velocity dependence of the total kinetic frictional force is modified in a velocity regime between the two crossover points ($0.7 \leq V \leq 4$). In this velocity regime, the velocity-weakening behavior of the kinetic frictional force due to the lower chain and the velocity-strengthening one due to the upper chain are complementary each other, and therefore the total kinetic frictional force becomes velocity-insensitive. It is found in both the cases that the results of the lowest order perturbation theory can explain excellently the behavior of the kinetic frictional force observed in the numerical simulations when the strength of the interchain interaction is less than the critical value of the Aubry transition. Therefore, it is confirmed also in the two-chain model that the lowest order perturbation is valid definitively in the absence of the Aubry transition, and then higher order contributions are quite negligible. Thus the lowest order perturbation gives us a correct and quite simple viewpoint on the kinetic frictional force of the two-chain model in the absence of the Aubry transition that the behavior of each chain can be understood as an individual deformable chain on the periodic potential and then the kinetic frictional force can be also composed of two contributions that come from such individual two chains. If

the Aubry transition exists in the two-chain model, such a simple viewpoint on two chains is modified largely and altered to a complicated one. Fig. 3(c) shows the kinetic frictional force for $K_s = 2$ in the case of strong interchain interaction, $K_I = 1$, which is the same strength as that in Fig. 1(b). There exists a obvious discrepancy between the result of the perturbation and that of the numerical calculation, but in a high velocity regime a good agreement is obtained. Such behavior is quite similar to that for the FK model in Fig. 1(b). Then we investigate the difference in the kinetic frictional force and the lattice structure between the FK model and the two-chain model. In particular, it is quite important to understand how the strong interchain interaction leads to the Aubry transition in two chains, and how both lattices behave in sliding states. In order to discuss lattice structures of two chains, we define two hull functions for the two chains of the present model in the following equations.

$$u_i = ic_a + Vt + h_a(ic_a + Vt), \quad (25)$$

$$v_i = ic_b + h_b(ic_b). \quad (26)$$

In this case the periodicity of the hull functions is expressed as

$$h_a(x) = h_a(x + c_b), \quad h_b(x) = h_b(x + c_a). \quad (27)$$

The sliding states of the strongly interacting two-chain model can also be analyzed using these two hull functions. Figs. 4(a)~(e) show the hull functions given by snapshots taken in the case of no external force and in steady sliding states at several velocities for the system with $K_I = 1$. For these model parameters, it should be noted that the Aubry transition occurs in the lower chain in the stationary state in the sense mentioned just below. It is confirmed from the fact that the hull function h_b in Fig. 4(a) shows the largest gap at the half of the period, $c_a/2 \approx 0.81$. On the other hand, the hull function for the upper chain is also much affected by the strong interchain interaction and have gap structure. But no gap exists at the half of the period, $c_b/2 = 0.5$. The state of the upper chain would be a sort of breaking of analyticity state, but we can distinguish that from the conventional Aubry's breaking of analyticity state for the FK model, which is characterized by the largest gap at the half of the period. The interchain force which affects the upper chain is not simple and spatially modulated because the lower chain is softer in elasticity than the upper one and is highly distorted. The atoms of the soft lower chain are bound near the minimum points of the almost periodic potential caused by the stiffer upper chain. This leads to the conventional Aubry's breaking of analyticity state in the lower chain. Thus, in the stationary state, the elasticities of two chains cause a peculiar breaking of analyticity state in each chain when the strength of the interchain interaction is greater than a critical value. The critical strength of the interchain interaction itself varies with

the elastic parameters as observed in Ref. [14]. These features of the hull functions are quite complicated and the perturbational treatment is apparently invalid in this case.

In sliding states with very low velocity, both the hull functions, h_a and h_b , retain the remainder of the gap structure and are highly distorted (Fig. 4(b)). As velocity increases, however, they gradually change their forms, approach to sinusoidal ones and reduce the amplitudes (Fig. 4(c)). Such behavior of the hull functions is essentially the same as that for the FK model. The sinusoidal form of the hull function h_b is almost recovered at $V \sim 0.658$ as seen in Fig. 4(d), but the hull function h_a is still distorted from the sinusoidal form. This difference in behavior between the two hull functions would come from the difference of their elasticities. For a higher velocity (Fig. 4(e)), both the hull functions become sinusoidal obviously. It is to be noted here that the main contribution to the kinetic frictional force comes from the lower chain, in which the conventional Aubry transition takes place as observed in Fig. 3(c). Hence the result of the numerical calculation on the kinetic frictional force comes closer to that of the perturbation theory above the velocity corresponding to Fig. 4(d), where h_b recovers sinusoidal form. Above the velocity corresponding to Fig. 4(e), where both hull functions become sinusoidal, they agree quite well. This means that the result of the numerical calculation for the two-chain model agrees well with that of the perturbation theory only when the effects due to the breaking of analyticity vanish in both chains and therefore the sinusoidal forms appear in both the hull functions.

Now we consider the conditions required for the validity of the lowest perturbation theory, Eqs. (20) and (21). Fig. 5 shows $\sqrt{\langle(\delta u_i)^2\rangle_i}/c_a$ (Eq. (20)) and $\sqrt{\langle(\delta v_i)^2\rangle_i}/c_b$ (Eq. (21)) as a function of velocity, where the parameters are the same as those in Fig. 4. In the small velocity regime $\sqrt{\langle(\delta u_i)^2\rangle_i}/c_a$ is quite small (≈ 0.06), but $\sqrt{\langle(\delta v_i)^2\rangle_i}/c_b$ is rather large (≈ 0.3). The large atomic displacement of the lower chain that is obtained by the lowest perturbation theory means that the theory itself is not valid although the atomic displacement of the upper chain calculated with the theory is quite small. In the high velocity regime above the characteristic velocities for two chains, which is about unity, the atomic displacements of both chains are suppressed and then the lowest order perturbation theory gives well description of the present system.

We discuss here the range of the parameters in which the present two-chain model is reduced to the FK model, i.e., a model that consists of a one-chain on a rigid periodic potential. This offers an interesting insight into the two-chain model because the importance of being the two chains is understood from it. In order to investigate the problem, we note the change of the gap structures of the

hull functions. Fig. 6 shows the two hull functions, h_a and h_b , in the absence of the external force for several K_s 's ($K_I = 1$ and $K_b = 0$). For small K_s ($K_s = 3$, Fig. 6 (a)), as observed also in Fig. 4(a), the central gap exists only in h_b , i.e., the conventional Aubry transition occurs in the lower chain. In this case the elasticity of the lower chain has great importance obviously because the lower chain has a dominant contribution to the kinetic frictional force. As K_s is increased ($K_s = 5$, Fig. 6 (b)), however, the central gap disappears in h_b . When K_s is increased further ($K_s \geq 10$, Figs. 6 (c) and (d)), the central gap appears in h_a . This is obviously contrary to those for small K_s 's, but this gap structure of h_a is just the same as that shown in Fig. 2 (a) for the Aubry transition in the FK model. Then the amplitude of h_b is strongly suppressed and all the gaps shrink. In this case the lower chain is very stiff, and its contribution to the frictional force is quite smaller than that from the upper chain in the low velocity regime. In the high velocity regime it is possible that the high-velocity-sliding upper chain excites high-frequency phonons in the stiff lower chain, and then a finite contribution to the kinetic frictional force from the lower chain is observable if the contribution from the upper chain is sufficiently small in this velocity regime. This is, of course, an essentially different point between the FK and two-chain models. If our discussion is restricted to the low velocity regime, the two-chain model can be reduced to the FK model in the large K_s regime, $K_s \gg 10$ for $K_I = 1$. Then, the maximum static and kinetic frictional forces become close to that for the FK model. Such behavior of the maximum static frictional force has been reported in Ref. [14]. The kinetic frictional force in such a case with the same values of the parameters with Fig. 3 (c), $K_I = 1$ and $K_b = 0$, but K_s , which is equal to 20, is shown in Fig. 7, where the lower chain is very stiff. The magnitude of the kinetic frictional force in the low velocity regime comes closer to that for the FK model in comparison with Fig. 3 (c). In the high velocity regime, however, the contribution from the stiff lower chain nevertheless becomes important. In Fig. 8 we summarize the characteristic parameter regimes for the two-chain model using the parameters, K_s and K_I . In the regime I, h_a shows the largest central gap, while there is no central gap in h_b , as observed in Figs. 6 (c) and (d). That is, as discussed above, the two-chain model is approximated by the FK model especially in the stationary and the low-velocity sliding states. In the regime II, however, no central gap exists in h_a and the gap structures of both the two hull functions become complicated. Then the contribution from the lower chain to the frictional force becomes important. The values of K_s at the boundary between the regimes I and II increase linearly with K_I . It is to be noted that there would be no exact phase boundary between the regimes I and II.

Thus the elasticity of two chains and the interchain interaction for the two-chain model affect each other com-

plexly when the strength of the interchain interaction is so strong that the Aubry transition occurs. Then the lowest order perturbation theory is not applicable to two-chain models in that case. Furthermore the feature characteristic of the two-chain model is more complicated than that for the FK model. It is found, however, that for both models the validity of the lowest order perturbation theory is retrieved in the high velocity regime, and the two-chain model is reduced to the FK model when the lower chain becomes stiffer than the upper chain under a certain condition on the strength of the interchain interaction.

VI. SUMMARY

We have investigated the kinetic frictional force for a one-dimensional two-chain model with an incommensurate lattice structure. On the basis of the explicit theoretical expression of frictional force, we have formulated a perturbation theory of the kinetic frictional force and clarified the contribution from the phonon excitation in each chain to the kinetic frictional force. From the study on the FK model (single deformable chain model) and the two-chain model we have found that the lowest order perturbation theory explains the numerical results excellently over a wide range of velocity if the strength of the interchain interaction is less than the critical value of the Aubry transition. Even if the finite static frictional force due to the Aubry transition appears, the lowest order perturbation theory is still valid in the high velocity regime where the suppression of atomic displacement becomes significant and the large lattice distortion due to the breaking of analyticity is reduced by high-velocity sliding motion. In particular, for the two-chain model with certain elastic parameters, we have found that the conventional Aubry's breaking of analyticity state, which is observed in the FK model and is characterized by the largest central gap of the hull function, and another breaking of analyticity state appear in the lower and upper chains, respectively. The latter lacks the largest central gap and is not well-defined in the context of the conventional Aubry transition. These stationary states cause complicated sliding lattice structures which are responsible for the discrepancy between the result of the perturbation theory and that of the numerical simulation. As velocity is increased, however, these states of two chains come to sliding states described by the lowest order perturbation theory. Thus, because each chain play an important role on the kinetic friction, it is necessary to take into account the contributions to the kinetic frictional force from both chains for understanding kinetic frictional force of the two-chain model [21].

We have also clarified the range of the parameters in which the two-chain model is reduced to the FK model. In the suitable range of K_I and K_s the former reduces to

the latter in the low-velocity regime. Even in that range, however, discrepancy between them appears in the high-velocity regime.

The present results for the two-chain model is useful to understand the earlier results in Refs. [14,17]. In these studies it was found numerically that the kinetic frictional force shows crossover behavior from velocity-strengthening to velocity-weakening and the crossover velocity and the strength of the kinetic frictional force are obviously different between the FK and two-chain models. Their results can be understood well with the perturbation theory of the present study.

In the present study the parameters of the model are chosen artificially and are not necessarily considered the correspondence to those in realistic materials because the system is one-dimensional. Actual frictional phenomena, however, take place in two- or three-dimensional systems. The effect of the three-dimensionality of phonon excitation and the elasticity in each substance would be crucial to the kinetic friction in such systems. Moreover, although the present model has no randomness, randomness such as impurities would affect the kinetic and static frictional forces. The relationship between the velocity dependence of the kinetic frictional force and the static frictional force caused by pinning due to such randomness is not well established. These issues will be discussed elsewhere [22].

ACKNOWLEDGMENTS

This work is financially supported by the Sumitomo Foundation and Grants-in-Aid for Scientific Research of Ministry of Education, Science, Sports and Culture.

-
- [1] F. P. Bowden and D. Tabor, *The Friction and Lubrication of Solids* (Clarendon Press, Oxford, 1954).
 - [2] G. Binnig, C. F. Quate, and Ch. Gerber, *Phys. Rev. Lett.* **56**, 930 (1986).
 - [3] J. Krim, *Comments on Cond. Mat. Phys. Part B* **17**, 263 (1995).
 - [4] B. N. J. Persson, *Comments on Cond. Mat. Phys. Part B* **17**, 281 (1995).
 - [5] *Physics of sliding friction*, B. N. J. Persson and E. Tosatti eds., (Kluwer Academic Publishers, Dordrecht, 1996).
 - [6] Y. Frenkel and T. Kontorova, *Zh. Eksp. Teor. Fiz.* **89**, 1340 (1938); **89**, 1349 (1938).
 - [7] S. Aubry, in *Solitons and Condensed Matter Physics*, Vol. 8 of *Springer Series in Solid-State Sciences*, A.R. Bishop and T. Schneider eds., (Springer, Berlin, 1978).
 - [8] H. Peyrard and S. Aubry, *J. Phys. C* **16**, 1593 (1983).
 - [9] S.N. Coppersmith, *Phys. Rev. B* **30**, 410 (1984).

- [10] S.N. Coppersmith and D.S. Fisher, *Phys. Rev. A* **38**, 6338 (1988).
- [11] J.B. Sokoloff, *Phys. Rev. B* **42**, 760 (1990), *J. Appl. Phys.* **72**, 1262 (1992).
- [12] M. Hirano and K. Shinjo, *Phys. Rev. B* **41**, 11837 (1990).
- [13] K. Shinjo and M. Hirano, *Surf. Sci.* **283**, 473 (1993).
- [14] H. Matsukawa and H. Fukuyama, *Phys. Rev. B* **49**, 17286 (1994).
- [15] E. Granato, M.R. Balcan and S.C. Ying, in *Physics of sliding friction*, B. N. J. Persson and E. Tosatti eds., (Kluwer Academic Publishers, Dordrecht, 1996).
- [16] T. Strunz and F.J. Elmer, in *Physics of sliding friction*, B. N. J. Persson and E. Tosatti eds., (Kluwer Academic Publishers, Dordrecht, 1996), M. Weiss and F.J. Elmer, *ibid.*
- [17] H. Matsukawa and H. Fukuyama, in *Physics of sliding friction*, B. N. J. Persson and E. Tosatti eds., (Kluwer Academic Publishers, Dordrecht, 1996).
- [18] Similar method is employed for the study of charge-density-wave dynamics. L. Sneddon, M.C. Cross and D.S. Fisher, *Phys. Rev. Lett.* **49**, 292 (1982). H. Matsukawa and H. Takayama, *J. Phys. Soc. Jpn.* **56**, 1507, (1987).
- [19] L. Sneddon, *Phys. Rev. Lett.* **52**, 65 (1984).
- [20] Similar behavior is also observed in infinite-dimensional model. D.S. Fisher, *Phys. Rev. Lett.* **50**, 1486 (1983) and *Phys. Rev. B* **31**, 1396 (1985). L. Sneddon, *Phys. Rev. B* **30**, 2974 (1984). H. Matsukawa and H. Takayama, *Solid State Commun.* **52**, 45, (1984).
- [21] Similar mechanism of the kinetic friction has been noticed also in a different context by Sokoloff. He considered a theoretical model of a microbalance experiment and discussed the kinetic friction between an adsorbed film and a three-dimensional substrate based on a perturbation theory. For a clean incommensurate interface, he found nearly equal contributions to the kinetic frictional force from the film and substrate. It is to be noted, however, his result is in an underdamped limit, in contrast to the present study. J.B. Sokoloff, *Phys. Rev. B* **51**, 15573 (1995).
- [22] T. Kawaguchi and H. Matsukawa, *Phys. Rev. B* **56**, 4261 (1997).

Fig. 1

Kinetic frictional force and averaged atomic displacement plotted against velocity (for the FK model). (a) A weak interchain interaction case: $K_I = 0.1$. (b) A strong interchain interaction case: $K_I = 1$. Marked and dotted lines represent the result of the numerical simulation and that of the perturbation theory, respectively. Solid line without marks denotes the averaged atomic displacement calculated with Eq. (20), which is renormalized by the mean lattice spacing.

Fig. 2

Hull functions for the FK model with strong interchain interaction $K_I = 1$. The velocities correspond to the figures are (a) 0 (no external force), (b) 2.03×10^{-2} , (c) 1.11×10^{-1} , (d) 3.95×10^{-1} , and (e) 3.22.

Fig. 3

Kinetic frictional force plotted against velocity (for the two-chain model). (a) and (b) correspond to a weak interchain interaction case $K_I = 0.1$, where only K_s is different: (a) $K_s = 2$ and (b) $K_s = 10$. (c) is for strong interchain interaction $K_I = 1$ and $K_s = 2$. Marked line represents the results of the numerical simulation. Solid line is the kinetic frictional force obtained by the perturbation theory, which is decomposed into the contribution from the upper chain (dotted line) and that from the lower chain (broken line).

Fig. 4

Hull functions for the two-chain model with strong interchain interaction ($K_I = 1$) and $K_s = 2$. The graphs in the left(right) row are the hull functions for the upper(lower) chain. The velocities are (a) 0 (no external force), (b) 1.36×10^{-2} , (c) 1.52×10^{-1} , (d) 6.58×10^{-1} , and (e) 1.33.

Fig. 5

Averaged atomic displacements plotted against velocity. The parameters are the same as those in Fig. 4. Solid and dashed lines represent $\sqrt{\langle(\delta u_i)^2\rangle_i}/c_a$ calculated with Eq. (20) and $\sqrt{\langle(\delta v_i)^2\rangle_i}/c_b$ calculated with Eq. (21), respectively.

Fig. 6

Hull functions for the two-chain model with strong interchain interaction $K_I = 1$. K_s 's chosen are (a) 3, (b) 5, (c) 10, and (d) 16.

Fig. 7

Kinetic frictional force plotted against velocity. Marked line with closed squares represents the results of the numerical simulation for $K_I = 1$ and $K_s = 20$. Marked line with open circles represents the results of the numerical simulation for the FK model with $K_I = 1$. Solid line is the kinetic frictional force obtained by the perturbation theory, which is decomposed into the contribution from the upper chain (dotted line) and that from the lower chain (broken line).

Fig. 8

Characteristic parameter regimes for the two-chain model. In the regime I, h_a shows the largest central gap, which is essentially the same as that for the FK model, and all the gaps of h_b highly shrink and no central gap exists there. In the regime II, no central gap exists in h_a , and both h_a and h_b show complicated gap structures.

Fig. 1(a) Kawaguchi and Matsukawa

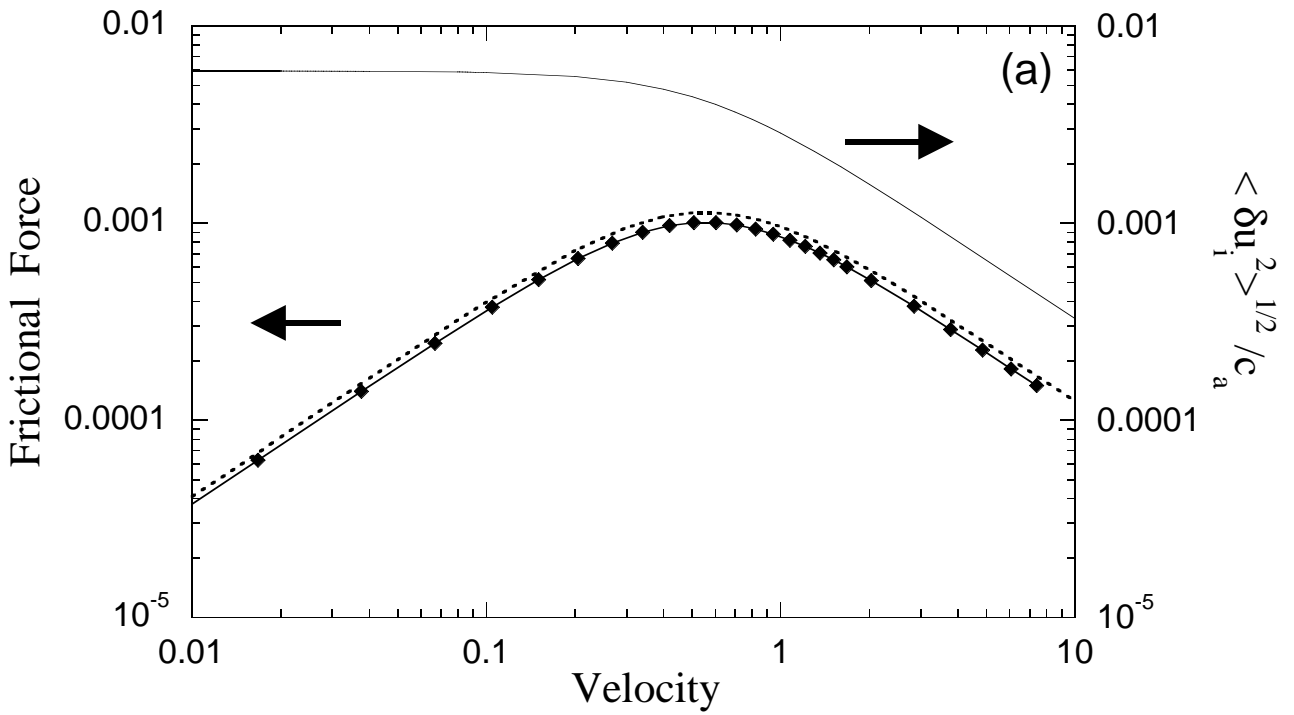
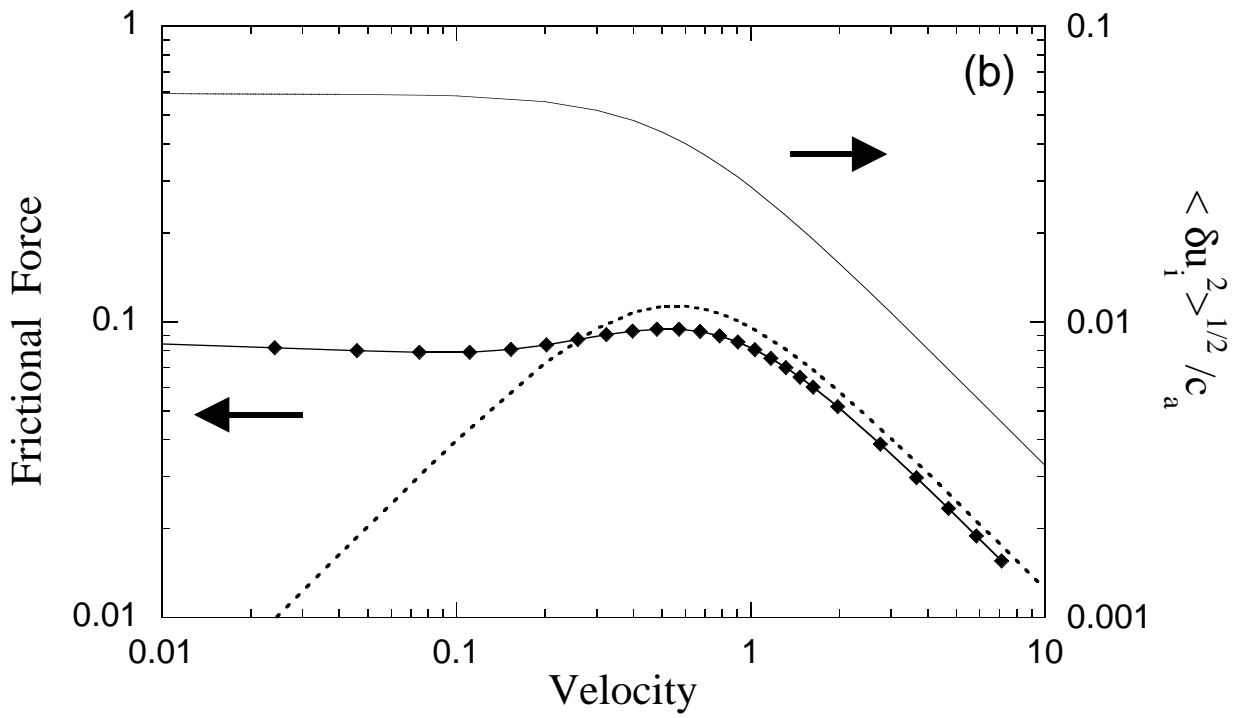


Fig. 1(b) Kawaguchi and Matsukawa



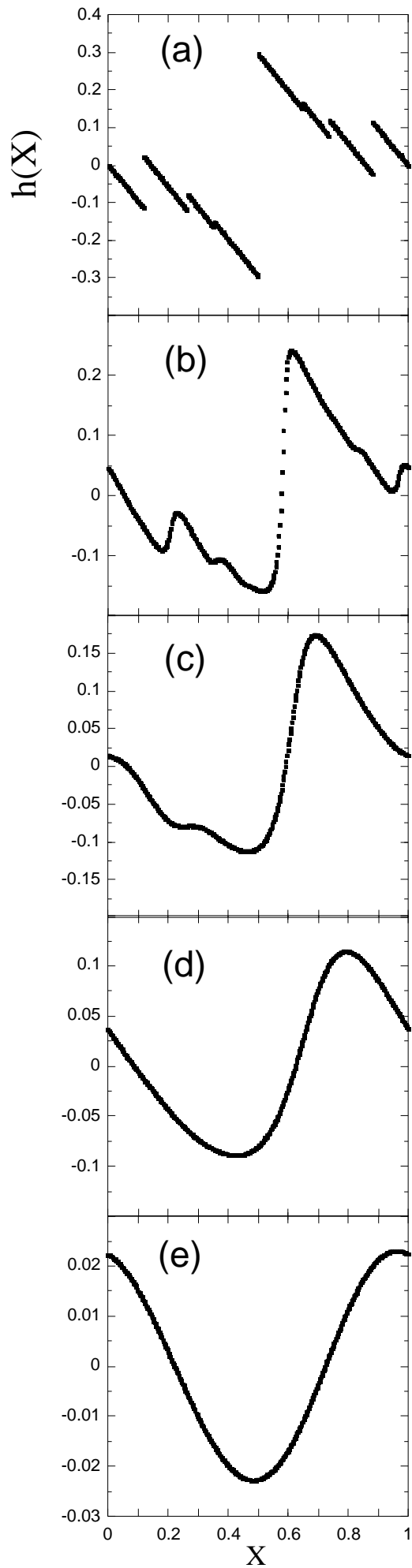


Fig. 2

Kawaguchi and Matsukawa

Fig. 3

Kawaguchi and Matsukawa

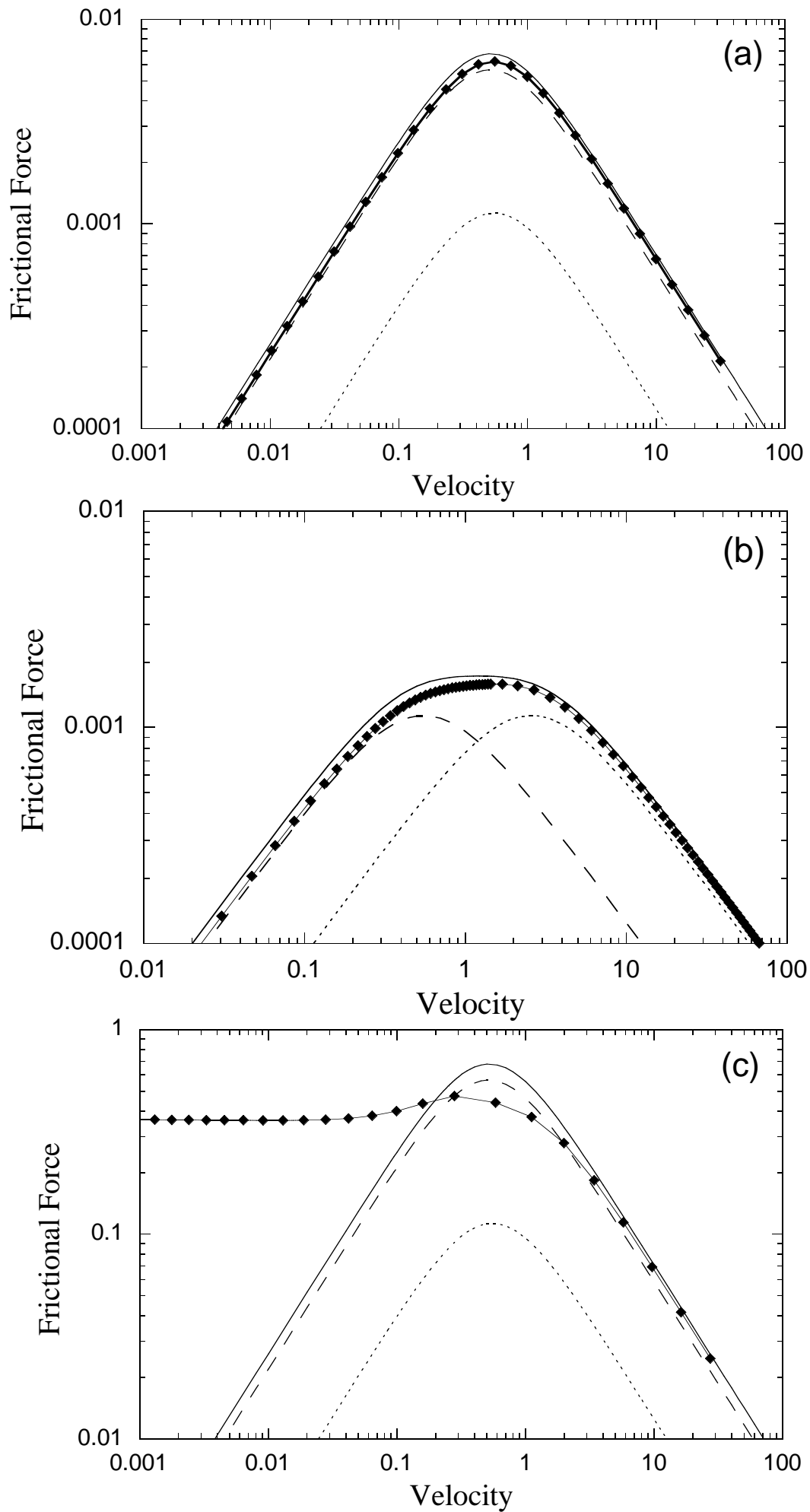


Fig. 4 Kawaguchi and Matsukawa

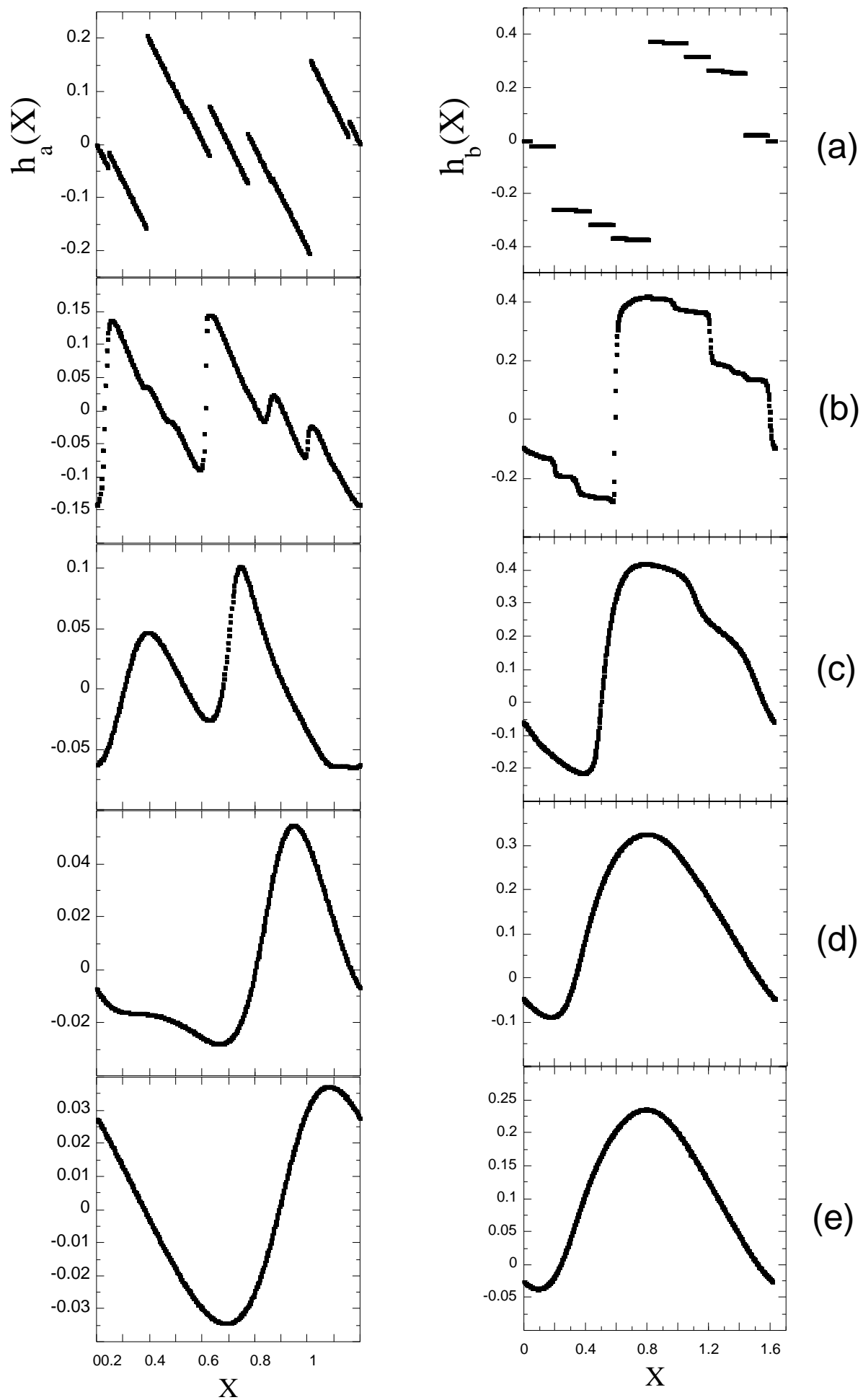


Fig. 5 Kawaguchi and Matsukawa

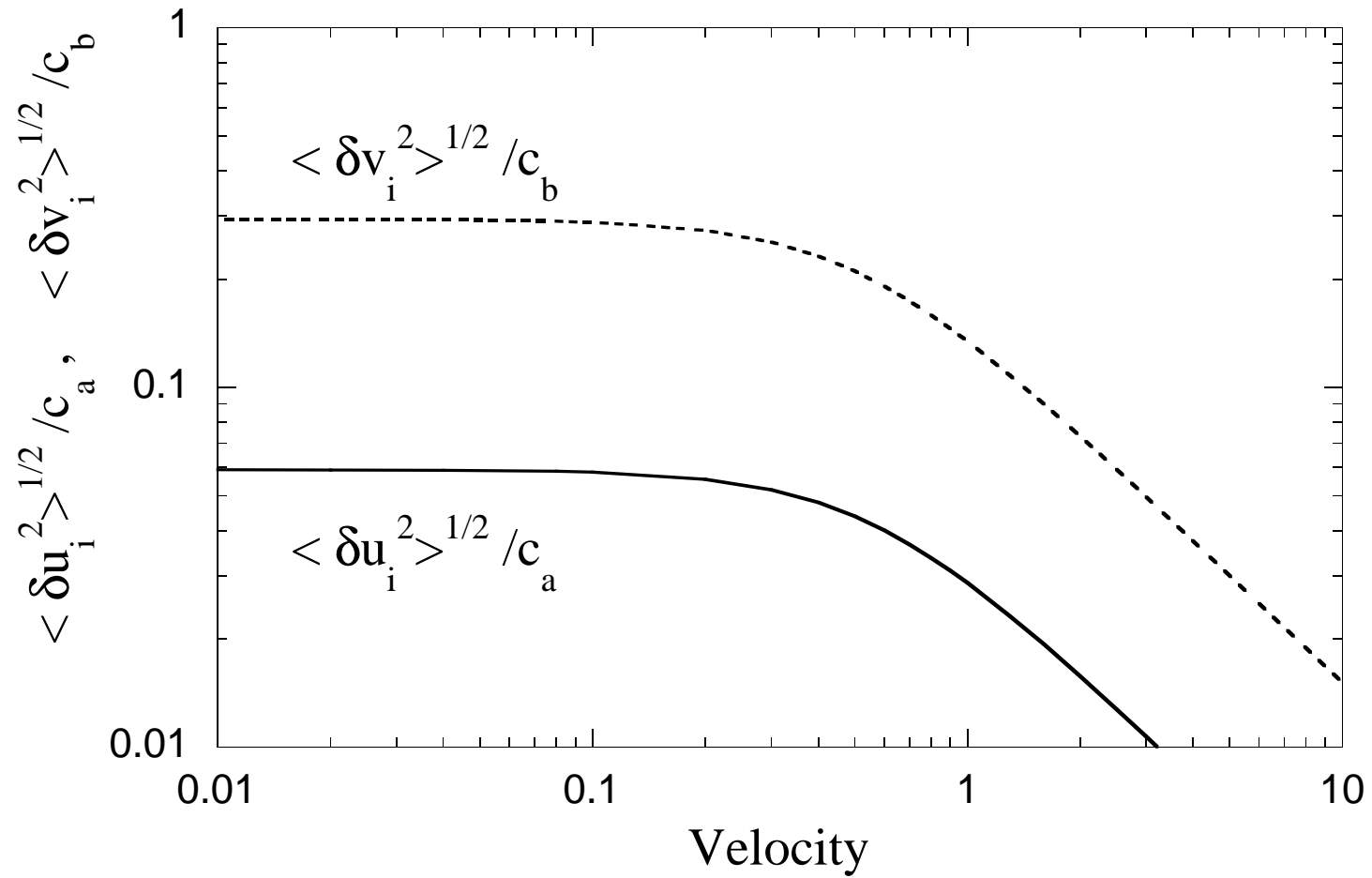


Fig. 6 Kawaguchi and Matsukawa

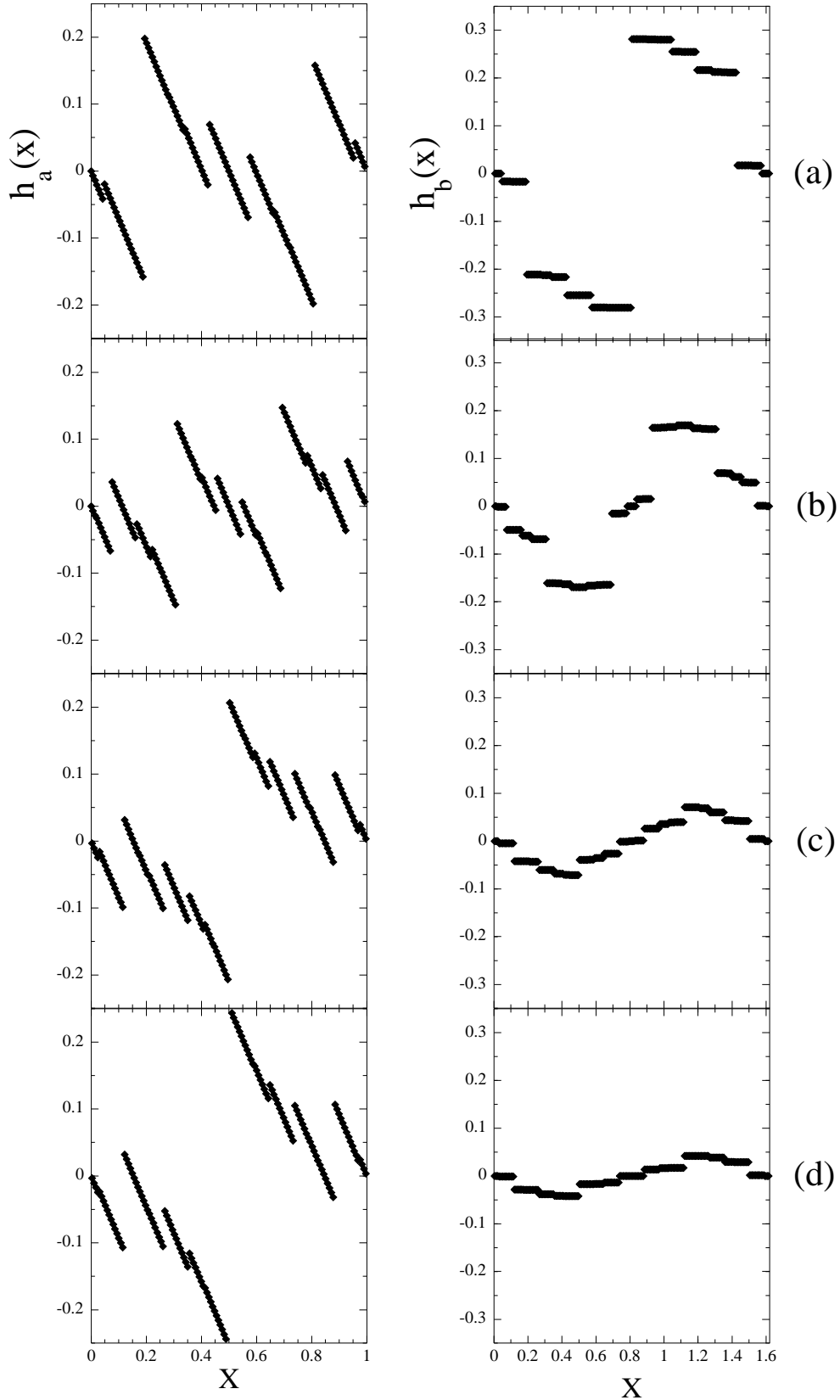


Fig. 7 Kawaguchi and Matsukawa

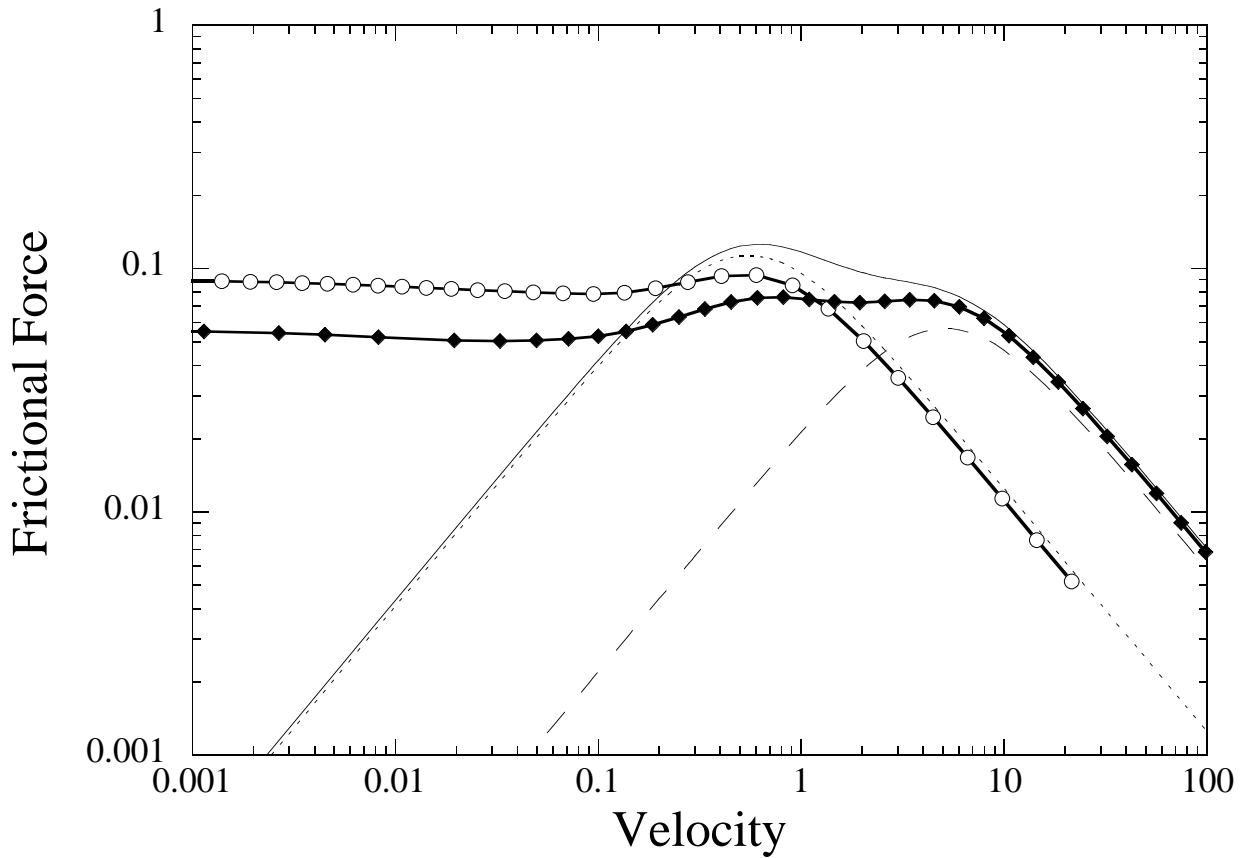


Fig. 8 Kawaguchi and Matsukawa

